Supporting Information for

Significant Production of Ozone from Germicidal UV Lights at 222 nm

Zhe Peng,[1,2] Douglas A. Day,[1,2] Guy Symonds,[1,2] Olivia Jenks,[1,2] Harald Stark,[1,2,3] Anne V. Handschy,[1,2] Joost de Gouw,[1,2] and Jose L. Jimenez[1,2]

1: Dept. of Chemistry, University of Colorado, Boulder, CO, USA
2: Cooperative Institute for Research in Environmental Sciences (CIRES), University of Colorado, Boulder, CO, USA
3: Aerodyne Research, Billerica, MA, USA

Supporting Information Text Sections

Section S1. Selection and Application of CBr_4 a tracer of GUV fluence rate in air

A useful chemical tracer of GUV exposure should not react (or react slowly) with common atmospheric oxidants such as O_3, OH, or the NO_3 radical at typical indoor air concentrations. O_3 and NO_3 typically react only with C=C double bonds, while OH can abstract hydrogens from most organic molecules.[1] A tracer should also have a high absorption cross section at the most common GUV wavelengths (222 and 254 nm), so that its decay is large enough and can be quantified over reasonable time scales despite instrumental noise. It should have high vapor pressure and low water solubility to reduce partitioning to room surfaces and tubing.[2,3] It should not be highly toxic, and it should be detectable with high sensitivity with existing instrumentation, so that its mixing ratio can be kept low to minimize any unwanted effects on chemistry or human exposure concerns. After comparing a few candidate species, we selected CBr_4 as a tracer. We show that it has relatively fast decay under 222 nm irradiation and can be detected by a commonly-available Proton-Transfer-Reaction Mass Spectrometer with high sensitivity.

A search for species with these properties that can serve as a GUV fluence rate tracer at both main GUV wavelengths in use (222 and 254 nm) identified three candidates, shown in the table below. Other species considered (including CF_2Br_2, CCl_3Br, CF_2I_2, C_2F_5I, CF_3I, OCS, and diacetyl) had too low absorption cross section (σ) at one of the key GUV wavelengths. CBr_4 was selected due to having the highest σ (and thus the fastest photolysis rates), low reactivity with oxidants, and being detectable with the Vocus instrument with high sensitivity. This instrument is widely-available in air chemistry research laboratories. This molecule is an excellent tracer in particular for GUV222, as its absorption cross section is highest at that wavelength, and falls about an order of magnitude when 10 nm away on either side of the peak. The absorption cross sections of CBr_4, O_2 and O_3 are shown in Fig. S6.

To quantify the sensitivity of the Vocus to CBr_4, 20.10 mg CBr_4 was evaporated under clean nitrogen flow into the chamber (whose volume was measured by quantitatively injecting CO_2 and measuring the concentration). A teflon-coated fan was run for one minute following the

addition to ensure complete mixing. The concentration of CBr_4 in the chamber and measured ion counts per second (cps) for the CBr_3^+ ion were used to determine the sensitivity in cps ppb^{-1}.

As CBr_4 also absorbs at 254 nm, it can cause interferences in the Thermo Scientific 49i O_3 Analyzer, which uses absorption at 254 nm to measure O_3. We measured the apparent O_3 signal in the Thermo Scientific 49i O_3 Analyzer at several CBr_4 concentrations in the absence of O_3 in the chamber. Below 200 ppb CBr_4, the interference of CBr_4 is approximately linear with its concentration (Fig. S11). The O_3 signal due to CBr_4 interference is ~0.007 ppb per ppb CBr_4 in this CBr_4 concentration range, in which most of the experiments in this study were (usually on the range 1-10 ppb). At very high CBr_4 concentration (~500 ppb), the relationship between the concentration and the O_3 interference is no longer linear.

During the O_3 generation rate quantification experiments, CBr_4 (Sigma-Aldrich) was added to the chamber after the O_3 quantification was done. This order was followed because CBr_4 photolysis produces Br radicals that can catalytically destroy O_3 in a similar way as catalytic destruction of stratospheric O_3 by Cl.[4] In the presence of CBr_4 and GUV irradiation (and hence Br atoms), a steady state for O_3 exists that is governed by Br concentration (and hence CBr_4 and GUV fluence rate). Fig. S12 shows the O_3-CBr_4 relationship during a long CBr_4 decay experiment with the Far UV fixture (with filter). CBr_4 decay was relatively slow. Therefore, O_3 concentration responded to CBr_4 relatively rapidly and could be regarded as steady-state concentration.

Table S1. key properties of potential GUV average fluence rate tracers. (*): Lifetimes are estimated for typical indoor GUV intensities of 2.61 x 10^{12} and 1.06 x 10^{14} photons cm^{-2} s^{-1} at 222 and 254 nm, respectively, and for an OH concentration of 1.5 x 10^6 molec. cm^{-3}. (**): no specific exposure limit, hazard information available at https://pubchem.ncbi.nlm.nih.gov/.

Species	CBr_4	$CHBr_3$	BrCOCOBr	CF_2Br_2	CCl_3Br	CF_2I_2	C_2F_5I	CF_3I
σ at 222 nm	2.85E-18	1.36E-18	2.00E-18	3.68E-19	4.60E-19	1.12E-18	4.73E-19	4.26E-19
σ at 254 nm	1.32E-17	5.78E-18	7.00E-18	2.44E-18	4.80E-19	6.00E-19	2.48E-20	2.06E-20
OH rate coeff.	-	2.70E-13	-	-	-	-	-	-
GUV-222 lifetime* (h)	8.0	18.4	15.2	43.5	221.4	177.0	4284	5158
GUV-254 lifetime* (h)	0.9	1.9	1.3	7.1	5.7	2.3	5.6	6.2
OH lifetime* (h)	-	686	-	-	-	-	-	-
Exposure limit (ppb)	100	500	**	10^5	**	**	**	**

Section S2. Selection of acetone as a tracer of Vocus sensitivity

A Vocus sensitivity tracer was useful for some experiments with weak lamps, e.g. the Naomi Wu (portable) and Eden Park (B) devices (Table 1), where the CBr_4 photolytic decay was small (~0.01 h^{-1}) and the Vocus sensitivity drift could be of a comparable magnitude.

Acetone was selected as a tracer of Vocus sensitivity because of the following properties. First, the Vocus instrument detects acetone with high sensitivity.[5] Besides, its absorption cross section drops by orders of magnitude between 195-200 nm and is 3-4 orders of magnitude lower than that of CBr_4 (Fig. S6), leading to little photolysis by the GUV band centered at 222 nm. Moreover, it is unreactive with O_3, and its reaction with OH is negligible under the conditions in this study. After injection into the chamber, the acetone signal can serve to continuously quantify small variations in Vocus sensitivity, for the experiments where the GUV device has the optical filter that filters the 190 nm band.

Section S3. Calibration of O_3 analyzers used for chamber and office experiments

O_3 formation in the chamber was always measured with a Thermo Scientific 49i O_3 Analyzer. That analyzer was calibrated using actinometry within the experimental chamber, where ~40 ppb of NO_2 was injected into the dry chamber, and the UVA lights are stepped through four discrete levels (between 10-100% of total UVA power). Equal amounts of NO and O_3 are generated, which are monitored with the O_3 analyzer and a Thermo Scientific 42i-TL NO-NO_2-NO_x Analyzer. The NO_x analyzer was calibrated using a NIST-certified (±2%) calibration standard (gas cylinder with NO in N_2) and Thermo Scientific Multi-Gas Calibrator (146i). We estimate that this method provides a calibration accuracy of ±5% for the O_3 analyzer.

O_3 decay rates and concentrations in the office experiments were always measured with a 2B Model 205 analyzer, which was cross-calibrated with the Thermo analyzer used in the chamber experiments, with its zero calibrated with zero air (resulting accuracy of ±7%, and zero uncertainty of ± 0.5 ppb).

Section S4. Data analysis and kinetic modeling for the office O_3 production experiment

Characterization Tests

In characterization tests (without a GUV lamp), the ventilation rate was measured as 0.52-0.61 hr^{-1} (τ: 1.6-1.9 h) using CO_2 decay. For initial characterization of O_3 decay, ~400-500 ppb O_3 were generated with an unfiltered low-pressure Hg lamp with partial emission at 185 nm (BHK 82-9304-03) (Fig. S3), together with CO_2 injection. As expected, the decay of O_3 generated by the Hg lamp was faster than CO_2 decay (Fig. S4), because of other O_3 losses than ventilation (dry deposition, reactions with VOC emitted indoors etc.). Subtracting the two rate coefficients yields an O_3 deposition coefficient of 0.76-1.1 h^{-1} (τ: 0.93-1.3 h), and the overall O_3 decay rate as 1.3-1.7 hr^{-1} (τ: 0.59-0.78 h).

Given the variability in these experiments, the CO_2 and O_3 decay rates were measured after each period in which the GUV lamp was turned on, as described in the main paper.

Modeling

To quantify the O_3 production rate from the GUV lamp, all relevant parameters affecting O_3 concentration in the office were modeled in KinSim. The first-order ventilation rate, first order deposition rate coefficient (implicitly including gas and aerosol reactions), and the approximate mixing ratio of O_3 entering the room from outside the room had to be measured or estimated.

The ventilation rate was directly measured using CO_2 pulse injection experiments discussed in the main paper, and the deposition rate was estimated by subtracting the ventilation rate from the first-order overall O_3 loss rate coefficient (green fit lines in Fig. S9). From here, the effective value for the O_3 mixing in from outside the room was approximated through tuning of the model when the lamp was off (blue points in Fig. S9). Finally, across 5 of the 8 peaks the production rate was tuned individually until it matched with each peak, and then the average was used as a constant production rate (individual values shown in Fig. S9 and used as a metric of uncertainty). Peaks 3, 7, and 8 were excluded due to rapidly changing O_3 background levels. As it was found that the estimated O_3 deposition rate varied substantially for the different light cycles, it was assumed to be constant for the model and the average value was used as an input (and computing "outside" O_3). This choice was made since, given the relative invariability of the ventilation rate and lack of activity in the room, it seemed unlikely that actual O_3 deposition rate coefficient would change all that much. More likely, the variability was more driven by a combination of uncertainty in changing ventilation rates and "outside" O_3 on timescales faster than these parameters could be quantified, as well as the uncertainties associated with fitting and subtracting decay and ventilation rates. Figure S9 displays all of these parameters in the first "variable deposition" scenario as well as the second "constant deposition scenario". The O_3 production rate for the GUV lamp was only calculated for the second scenario.

As seen in Fig. S10, The O_3 production rate for the conference room is slightly lower than that of the chamber due to the size of the room (~32.9 vs. ~20.6 m^3) and effective UV pathlength (~3.2 vs. ~4.5 m). However, the results are within error bars when these differences are taken into account. The effective path length is shorter in the conference room both because of the shorter length of the room (3.8 m), and the combination with the narrowness of the room and furniture obstructions, which we estimate to reduce effective pathlength by ~15%.

Section S5. Evaluation of handheld electrochemical O_3 monitors

Three low-cost (~$100) handheld electrochemical O_3 monitor models were compared with our research-grade UV absorption Thermo Scientific Model 49i Ozone Analyzer. Table S2 lists all three monitors with their relevant information and specs. Two identical monitors were tested for the Shenzhen Dienmern model.

Table S2. Specifications for all low-cost O_3 monitors tested in the chamber instrument

Company and cost	Name, Model, and Principle of Operation	Advertised Specifications	Resolution of Monitor Display
Shandong Renke Control Technology Co., Ltd. $114	"Portable Accurate O3 Sensor" Model: RS-MG41-O3 Electrochemical sensor	0~10.00 ppm Accuracy: ±6%FS(@5ppm,25℃,50% RH) Zero drift: ≤±1ppm Duplicate Value: ≤2% From listing on Renke's website: https://www.renkeer.com/product/portable-ozone-meter/	0.01 ppm (10 ppb)
Shenzhen Dienmern Testing Technology Co., Ltd $55	"Portable O3 handheld gas analyzer" Model: DM509-O3 model Electrochemical sensor	O_3(0-5 ppm) From listing on Alibaba.com: https://dienmern.en.alibaba.com/product/1600275994341-910743044/Portable_Ozone_Analyzer_Hing_accurate_O3_Ozone_sensor_Air_Detector_Intelligent_Sensor_Ozone_Meter_Air_Quality_Pollution_Monitor.html?spm=a2700.shop_index.111720.3.55b15bceN6NeQC	0.001 ppm (1 ppb)
Shenzhen YuanTe Technology Co., Ltd $815	"Portable Gas Detector" Model: SKY2000 Electrochemical sensor	0-10 ppm Accuracy: ≤±3% F.S. Repeatability: ≤±1% Linearity Error: ≤±1% Zero Shift: ≤±1% (F.S./year) https://siafa.com.ar/media/src/sky2000-catalogue-with-datasheetam.pdf https://www.ato.com/portable-o3-gas-detector?affiliate=shopping&gclid=CjwKCAjwx_eiBhBGEiwA15qLN6lkKk3nanBn5ZAzfqL5ereO0HcjlOLdUMcFdqNlEI_3Qk5f47it2RoCRVcQAvD_BwE	0.01 ppm (10 ppb)

The set up for these monitors in the chamber can be seen in Fig. S13. O_3 was injected into the chamber with a commercial O_3 generator (BMT 802N) periodically, followed by mixing with a fan, in order to generate constant concentration O_3 "steps". The Thermo O_3 concentrations were logged continuously and the concentrations of the hand-held O_3 monitors were manually read and recorded for each step. The results of this comparison can be seen in Figs. S14 and S15.

Performance is very poor at the relevant levels for typical indoor O_3 and the levels expected when GUV222 is applied at e.g. ACGIH limits (i.e. no response for O_3 <150–400 ppb). At higher levels > 200 ppb, the Shenzhen YuanTe monitor eventually quantifies O_3 with good accuracy, while the other two models continue to be low by a factor of ~8. The Shenzhen YuanTe monitor is also distinct from the other two as it is a factor of ~10 more expensive. According to the information that we could find (see Table S2), two of these monitors appear to have failed their accuracy and/or zero drift specifications. For the other one, the only specs that we found were the measurement range and statements that it has high accuracy. To the best of our current knowledge, the lowest cost monitors capable of accurate O_3 measurements at single-digit or tens of ppb-level concentrations are based on UV absorption, and cost at least $6000.

Section S6. Comparison of the health effects (premature death) for O_3 and fine PM.

The mortality due to long-term exposure to O_3 (per unit mass of O_3) can be estimated from the literature. Turner et al. (2016)[6] is considered the best study to date on this topic (J. Balmes, UCSF, pers. comm., 2023). This study reports an increase in all-cause mortality of 2% per 10 ppb increase in O_3. 10 ppb are equivalent to 19.7 μg m^{-3} at 1 atm and 298 K. Thus, we can estimate the risk per unit mass of O_3 as 2% / 19.7 = 0.10% per μg m^{-3}.

For comparison, the mortality due to long-term exposure to $PM_{2.5}$ can be estimated from Figure 2a of Weichenthal et al. (2022)[7]. For their updated exposure function, the increased relative risk of mortality per unit increase in $PM_{2.5}$ (i.e. the slope of the curve) is highest between 2.5-4 μg m^{-3}, at about 3.2% per μg m^{-3}. At concentrations around the US $PM_{2.5}$ average of ~7 μg m^{-3}, this value is 1% per μg m^{-3} for their updated function, and 0.95% per μg m^{-3} for the prior literature function.

Thus depending on the estimate used for $PM_{2.5}$ risk, the all-cause mortality risk of $PM_{2.5}$ is 9.5-32 times larger than for O_3.

References:

(1) Atkinson, R.; Arey, J. Atmospheric Degradation of Volatile Organic Compounds. *Chem. Rev.* **2003**, *103* (12), 4605–4638.
(2) Pagonis, D.; Price, D. J.; Algrim, L. B.; Day, D. A.; Handschy, A. V.; Stark, H.; Miller, S. L.; de Gouw, J.; Jimenez, J. L.; Ziemann, P. J. Time-Resolved Measurements of Indoor Chemical Emissions, Deposition, and Reactions in a University Art Museum. *Environ. Sci. Technol.* **2019**, *53* (9), 4794–4802.
(3) Liu, X.; Deming, B.; Pagonis, D.; Day, D. A.; Palm, B. B.; Talukdar, R.; Roberts, J. M.; Veres, P. R.; Krechmer, J. E.; Thornton, J. A.; de Gouw, J. A.; Ziemann, P. J.; Jimenez, J. L. Effects of Gas–wall Interactions on Measurements of Semivolatile Compounds and Small Polar Molecules. *Atmos. Meas. Tech.* **2019**, *12* (6), 3137–3149.
(4) Seinfeld, J. H.; Pandis, S. N. *Atmospheric Chemistry and Physics: From Air Pollution to Climate Change*; John Wiley & Sons, Inc.: Hoboken, NJ, USA, 2006; p 1232.
(5) Pagonis, D.; Sekimoto, K.; de Gouw, J. A Library of Proton-Transfer Reactions of H3O+ Ions Used for Trace Gas Detection. *J. Am. Soc. Mass Spectrom.* **2019**, *30* (7), 1330–1335.

(6) Turner, M. C.; Jerrett, M.; Pope, C. A., 3rd; Krewski, D.; Gapstur, S. M.; Diver, W. R.; Beckerman, B. S.; Marshall, J. D.; Su, J.; Crouse, D. L.; Burnett, R. T. Long-Term Ozone Exposure and Mortality in a Large Prospective Study. *Am. J. Respir. Crit. Care Med.* **2016**, *193* (10), 1134–1142.
(7) Weichenthal, S.; Pinault, L.; Christidis, T.; Burnett, R. T.; Brook, J. R.; Chu, Y.; Crouse, D. L.; Erickson, A. C.; Hystad, P.; Li, C.; Martin, R. V.; Meng, J.; Pappin, A. J.; Tjepkema, M.; van Donkelaar, A.; Weagle, C. L.; Brauer, M. How Low Can You Go? Air Pollution Affects Mortality at Very Low Levels. *Sci Adv* **2022**, *8* (39), eabo3381.
(8) Claus, H. Ozone Generation by Ultraviolet Lamps†. *Photochem. Photobiol.* **2021**, *97* (3), 471–476.
(9) Yoshino, K.; Esmond, J. R.; Cheung, A. S.-C.; Freeman, D. E.; Parkinson, W. H. High Resolution Absorption Cross Sections in the Transmission Window Region of the Schumann-Runge Bands and Herzberg Continuum of O2. *Planet. Space Sci.* **1992**, *40* (2), 185–192.
(10) Burkholder, J. B.; Sander, S. P.; Abbatt, J. P. D.; Barker, J. R.; Cappa, C.; Crounse, J. D.; Dibble, T. S.; Huie, R. E.; Kolb, C. E.; Kurylo, M. J.; Others. *Chemical Kinetics and Photochemical Data for Use in Atmospheric Studies; Evaluation Number 19*; Pasadena, CA: Jet Propulsion Laboratory, National Aeronautics and Space …, 2020. https://trs.jpl.nasa.gov/handle/2014/49199.

Supporting Information Figures

Figure S1. Pictures showing the FarUV GUV222 lamp mounted inside the Teflon chamber. Other lamps were tested in the same physical configuration. All tests were performed with the visible lights off, as in the last picture.

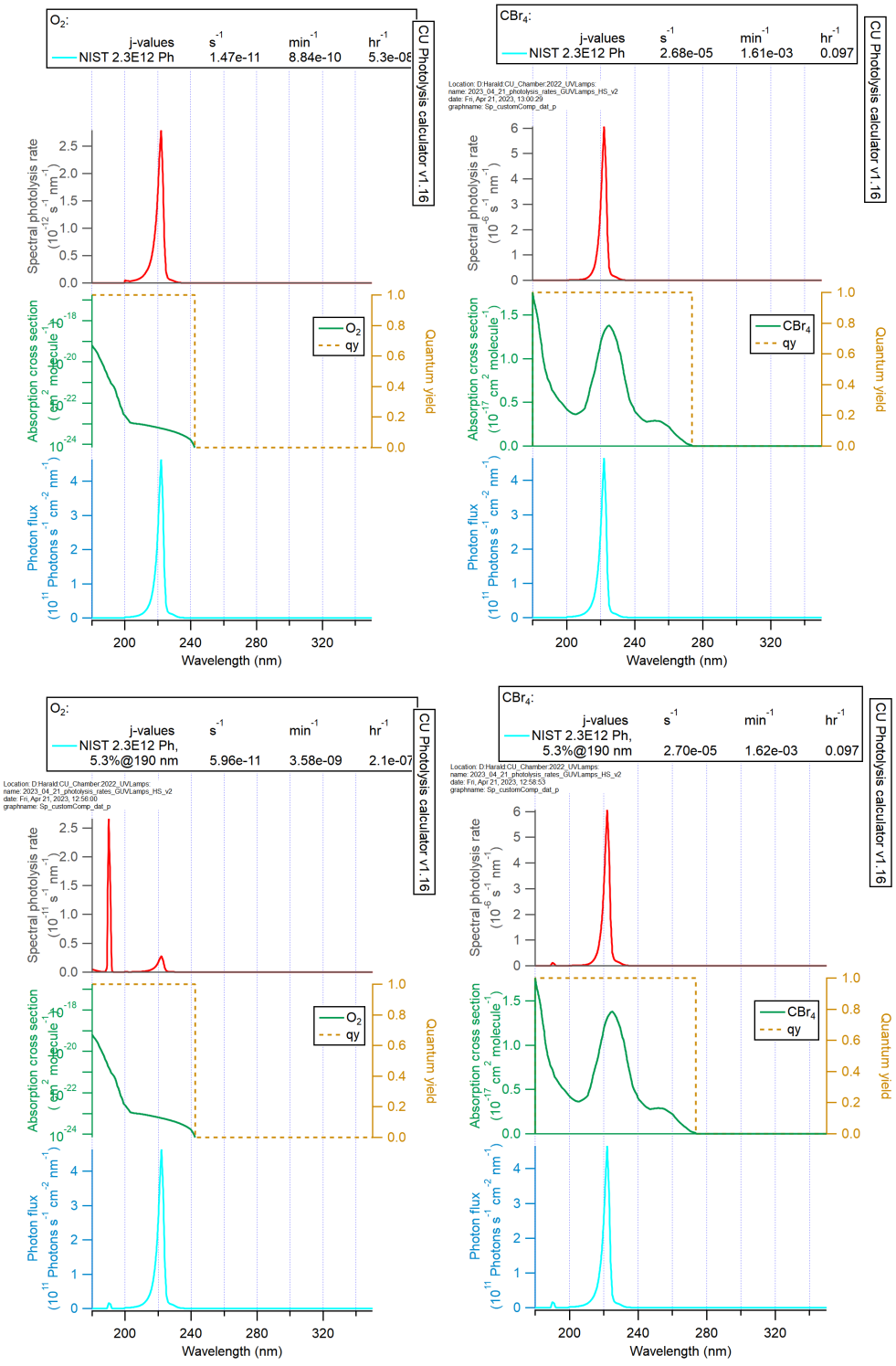

Figure S2. (Top) photolysis spectra and rates from O_2 (left) and CBr_4 (right) for NIST-measured Ushio lamp spectrum. (Bottom) results for the same lamp with an additional peak of 5.3% of the peak intensity manually added centered at 190 nm, estimated from Claus (2021).[8] These results were generated with the CU-Boulder photolysis calculator.

Figure S3. Experimental setup in the test office. The O_3 sampling tube and CO_2 injection tube were placed in the middle of the room on a ring stand (left). The GUV lamp was placed high in the room against the West wall of the room (right). The path of the light was interrupted by the furniture and walls, and the effective pathlength in the main paper was estimated to account for those obstructions.

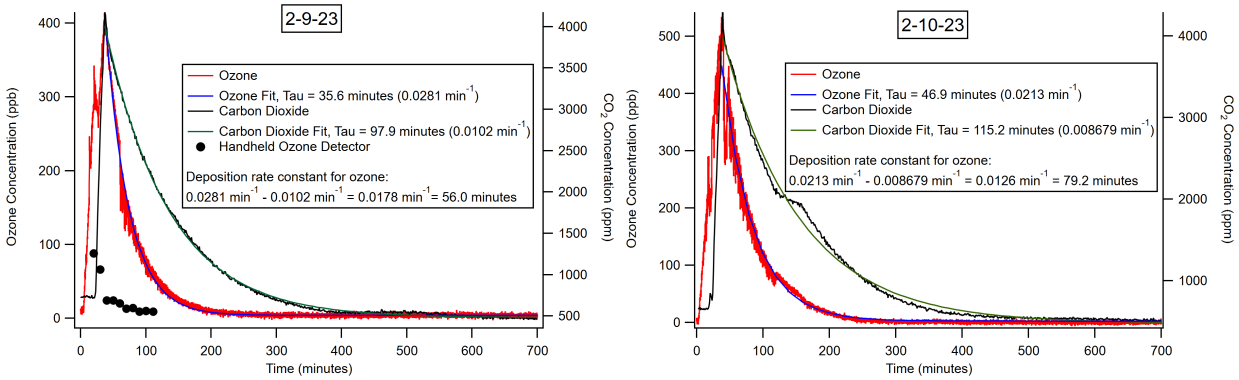

Figure S4. Decays of O_3 and CO_2 in the office experiments, along with the approximate decay first-order rate coefficients for 2 experiments on 2 different days. Measurements from a handheld low-cost O_3 detector are also shown, which underestimated the O_3 concentration by about an order-of-magnitude (see Section S5).

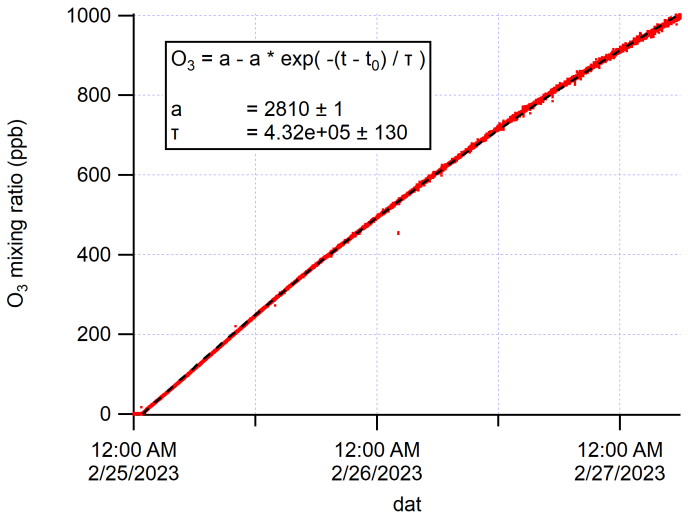

Figure S5. O_3 concentration vs. time in the chamber when the custom lamp with an Ushio B1 module was turned on for an extended period.

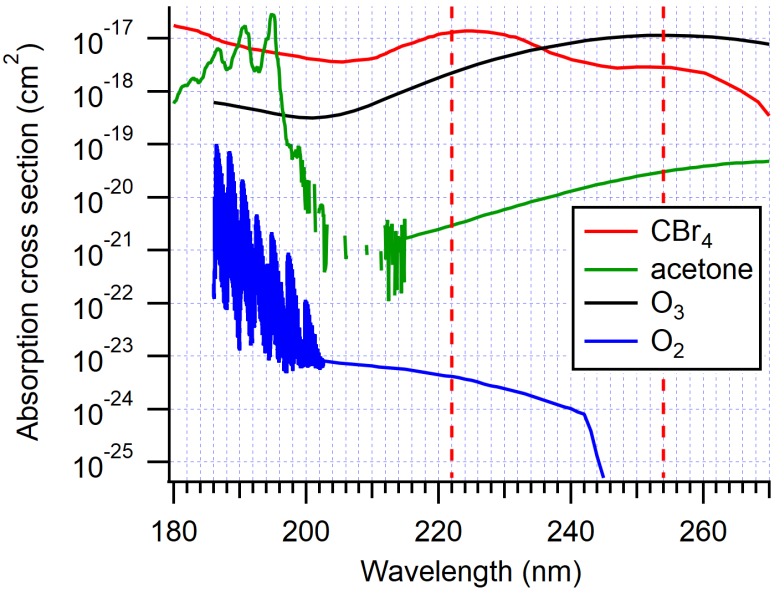

Figure S6. Absorption cross sections vs. UV wavelength for O_2, O_3, acetone and CBr_4.[9,10]

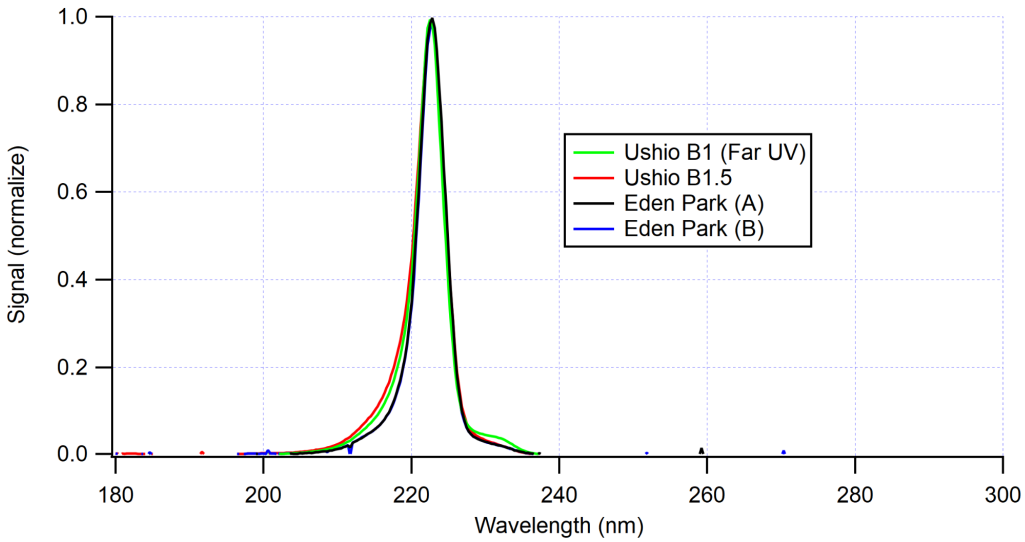

Figure S7. Measured emission spectra of the Far UV (Ushio B1), Ushio B1.5, and Eden Park (A) and (B) lamps. All spectra were measured with their original filters in place.

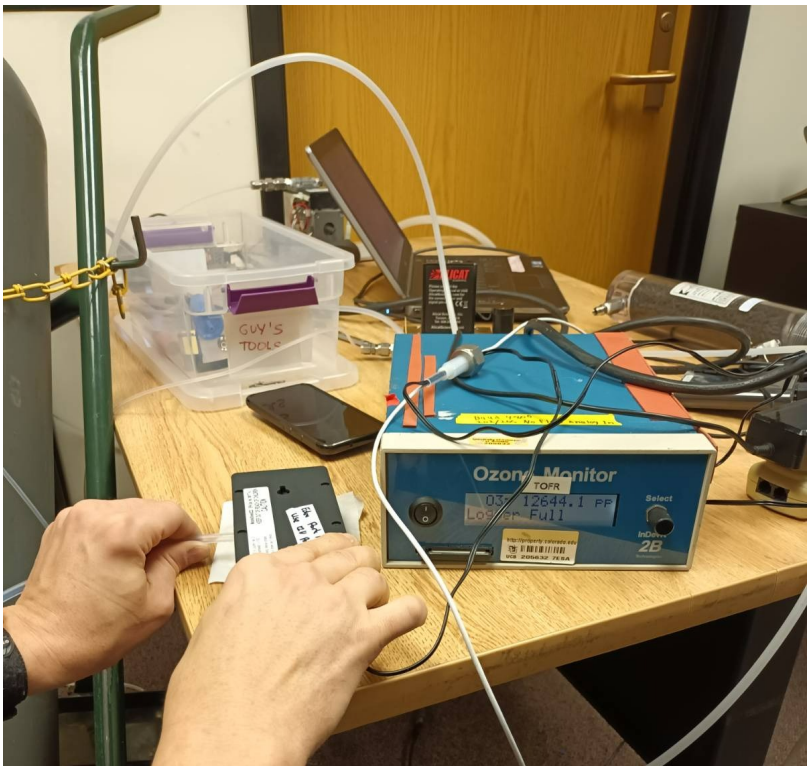

Figure S8. Picture of the setup for O_3 measurement just outside the electronics compartment of the Eden Park (A) device (black box held with right hand). The light emission surface points down into the table. The 2B O_3 analyzer displays a measured O_3 concentration of 12.6 ppm. Similar readings were observed for a period of several minutes.

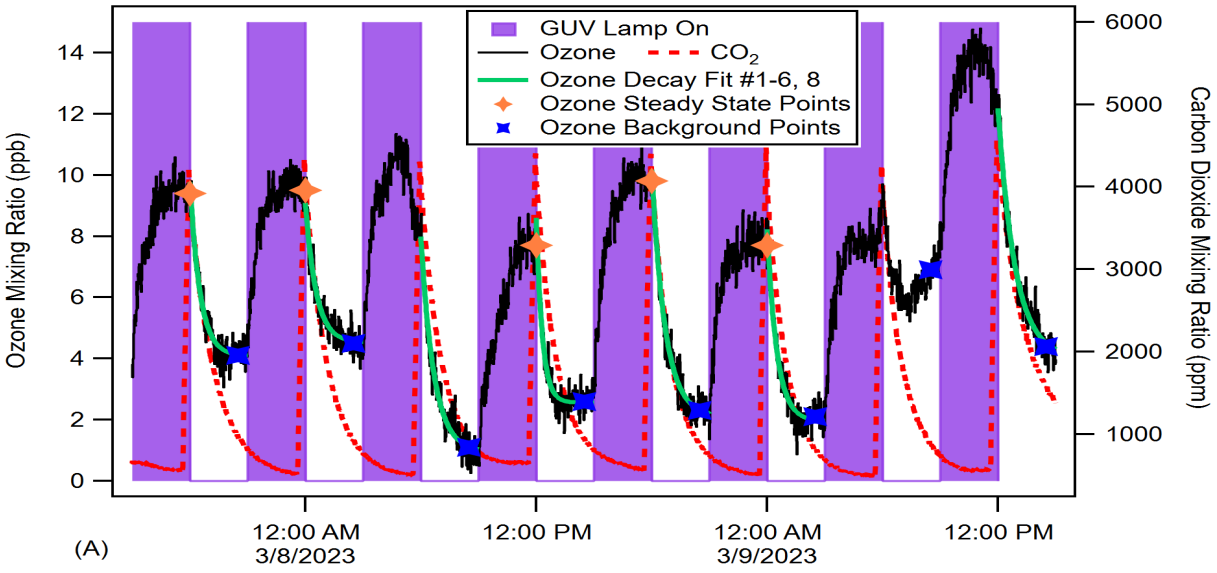
GUV Lamp On
Ozone
CO_2
Ozone Decay Fit #1-6, 8
Ozone Steady State Points
Ozone Background Points
Ozone Mixing Ratio (ppb)
Carbon Dioxide Mixing Ratio (ppm)
0
2
4
6
8
10
12
14
1000
2000
3000
4000
5000
6000
12:00 AM
3/8/2023
12:00 PM
12:00 AM
3/9/2023
12:00 PM
(A)

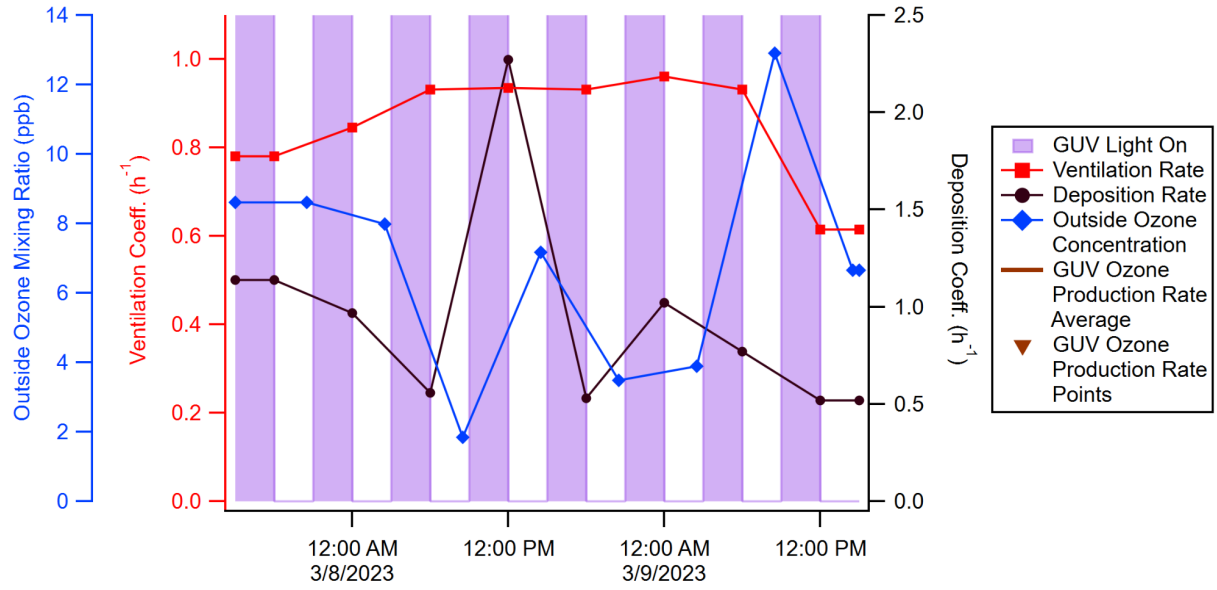
Outside Ozone Mixing Ratio (ppb)
Ventilation Coeff. (h^{-1})
Deposition Coeff. (h^{-1})
0
2
4
6
8
10
12
14
0.0
0.2
0.4
0.6
0.8
1.0
0.0
0.5
1.0
1.5
2.0
2.5
12:00 AM
3/8/2023
12:00 PM
12:00 AM
3/9/2023
12:00 PM
GUV Light On
Ventilation Rate
Deposition Rate
Outside Ozone Concentration
GUV Ozone Production Rate Average
GUV Ozone Production Rate Points

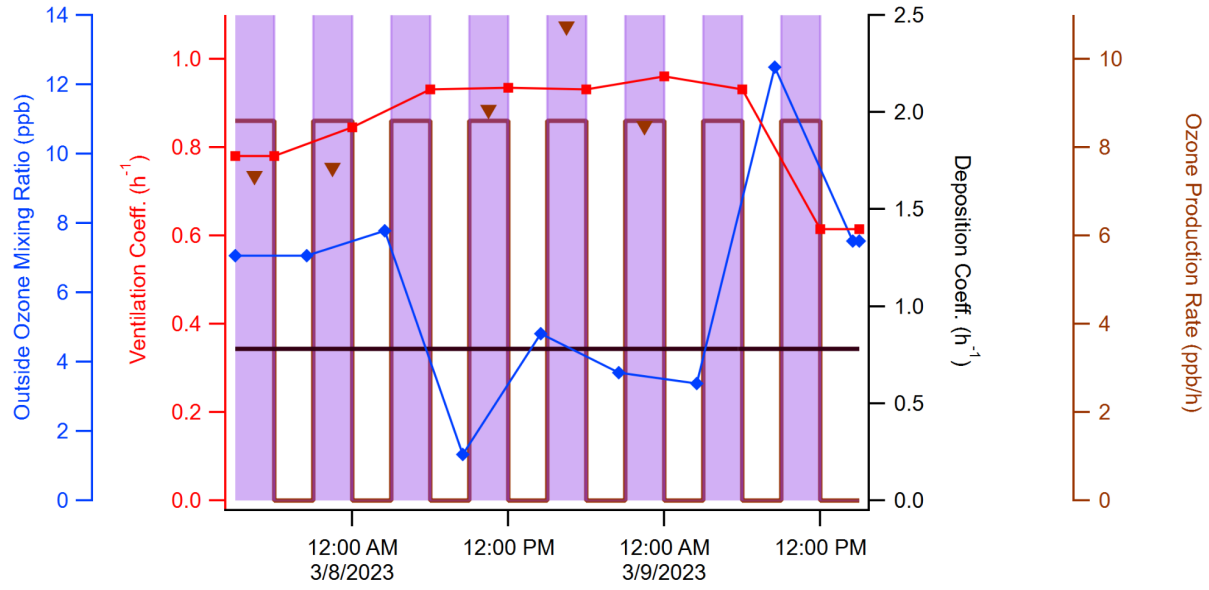

Figure S9. (Top): O_3 concentration in the office as the GUV lamp was cycled on and off in 3-hour increments over 8 total cycles with corresponding CO_2 pulses to measure ventilation rate. (Middle and Bottom): relevant parameters for modeling O_3 concentrations in the office experiments with the KinSim model, plotted vs. time. The middle graph shows the scenario where deposition varies over time. The bottom graph shows the scenario where deposition is assumed to be constant.

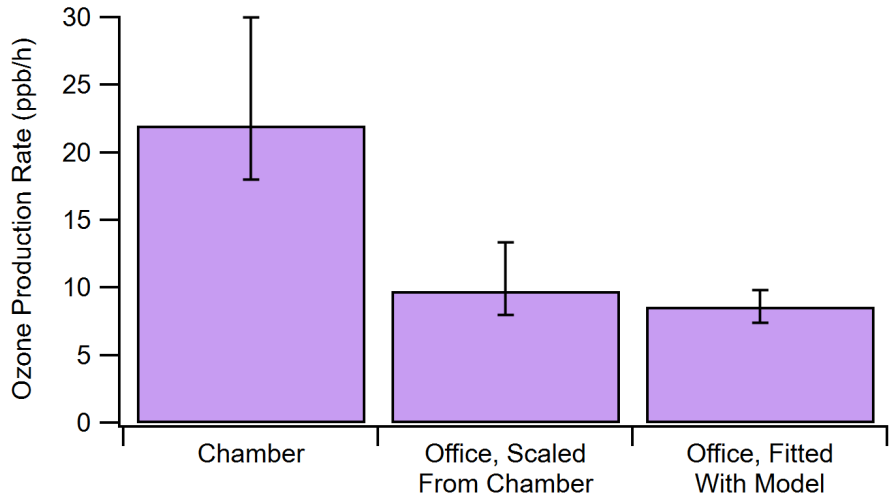

Figure S10. The production rates of O_3 compared between the conference room and chamber along with the value expected for the conference room by scaling the chamber results with the relative room volume and effective GUV light pathlengths.

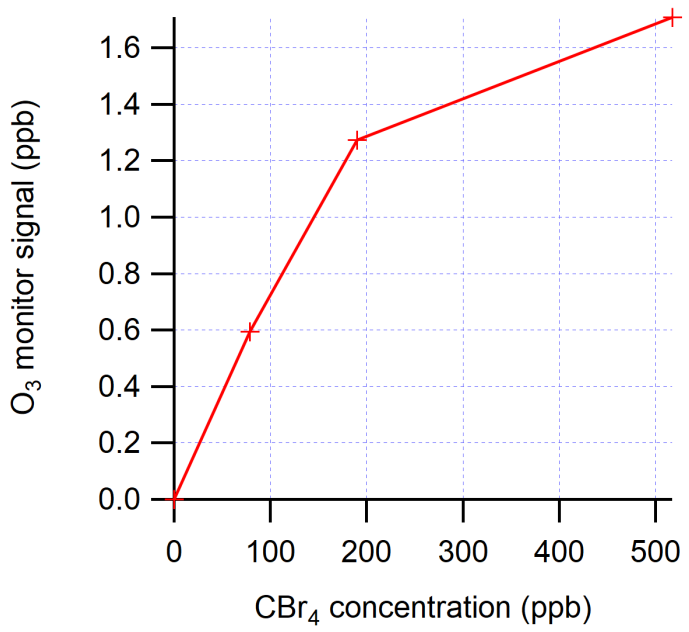

Figure S11. Apparent O_3 signal measured in the chamber due to CBr_4 interference at different CBr_4 concentrations.

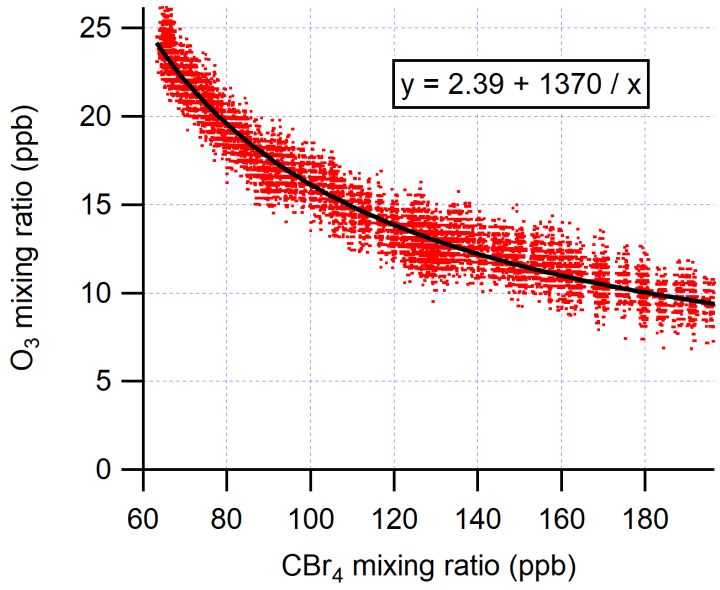

Figure S12. Evolution of O_3 and CBr_4 concentrations during a CBr_4 photolysis experiment with the Far UV lamp (Ushio B1) lasting 12 h.

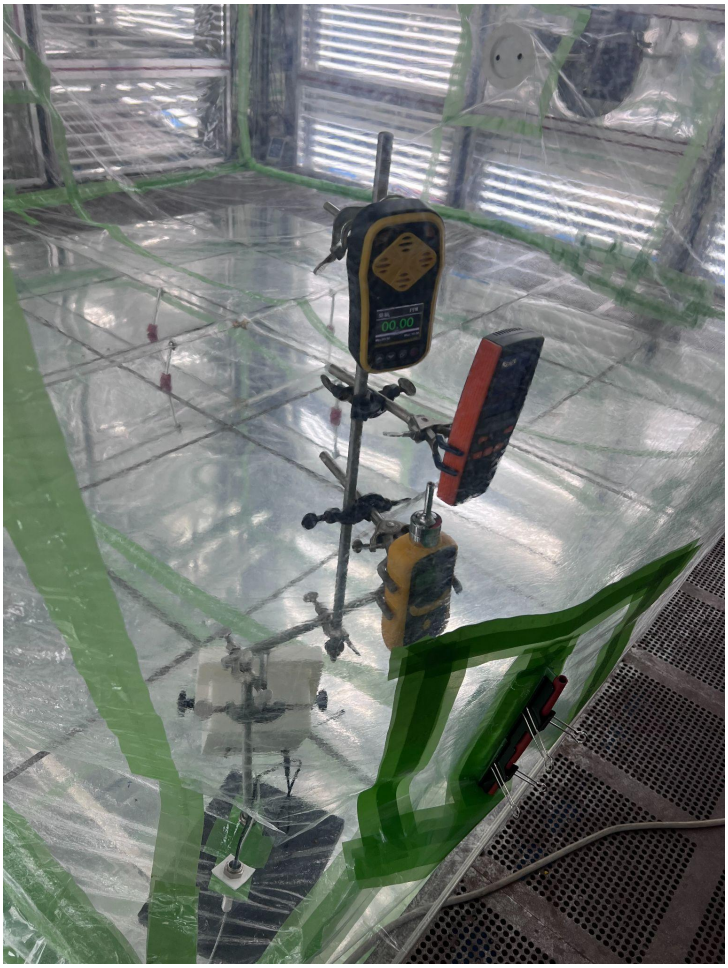

Figure S13. Set up with three handheld O_3 monitors inside of the chamber. The Shandong Renke model is on top, the Shenzhen Dienmern model is in the middle, and the Shenzhen YuanTe model is on the bottom.

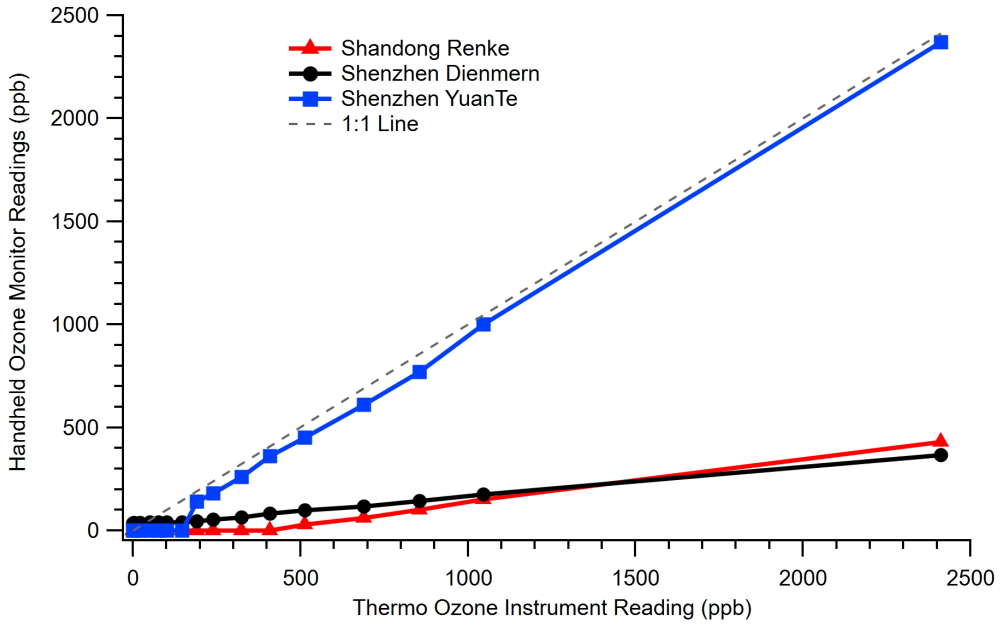

Figure S14. Comparison of the three portable O_3 monitors against the research-grade Thermo O_3 instrument.

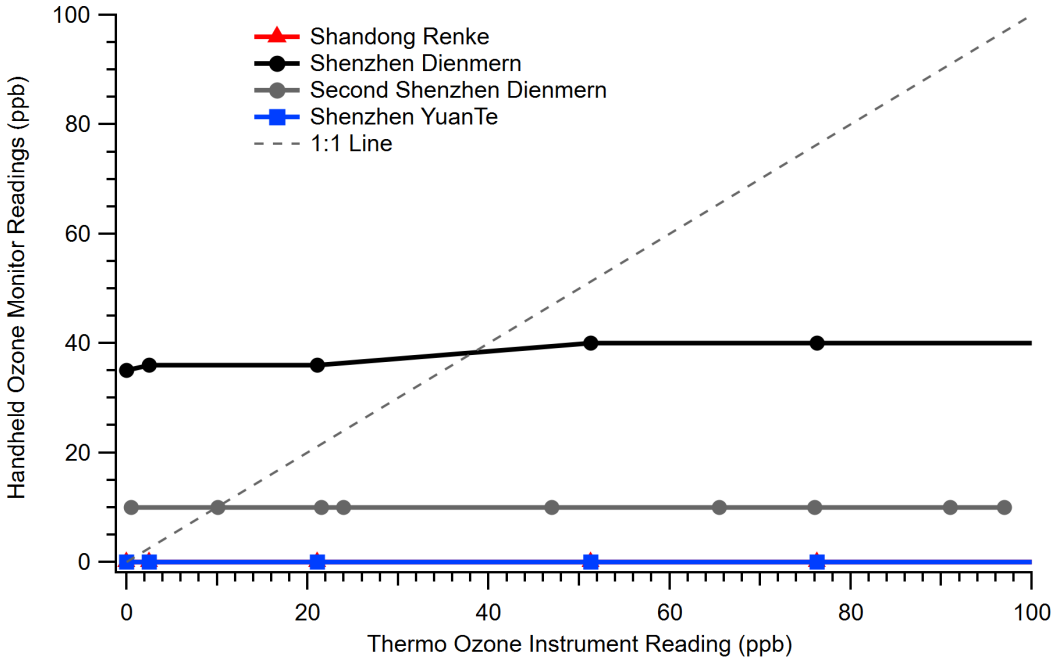

Figure S15. Comparison of the three portable O_3 monitors against the research-grade Thermo O_3 instrument, zoomed in the range of 0-100 ppb. A second and identical model Shenzhen Dienmern was also tested and shown in the gray line. This test was repeated once and none of the monitors showed appreciable differences, even the Shenzhen YuanTe still registered 0.00 ppm O_3 (while being exposed to values in the range of this graph) after a zero calibration inside the clean O_3-free chamber.